Secondary Structure of the Self-Cleaving RNA of Hepatitis Delta Virus: Applications to Catalytic RNA Design†

Michael D. Been,* Anne T. Perrotta, and Sarah P. Rosenstein

Department of Biochemistry, Box 3711, Duke University Medical Center, Durham, North Carolina 27710

Received July 31, 1992; Revised Manuscript Received September 3, 1992

ABSTRACT: A model for the secondary structure of the self-cleaving RNA from hepatitis delta virus was tested. Specific base changes were introduced in each of four regions with the potential for base-pairing (stems I–IV), and for each variant sequence, a rate constant for cleavage was determined. In each stem, mutations that would interfere with Watson–Crick base-pairing also reduced the first-order rate constants by 10–10^4-fold relative to the unmodified version. Within stems I and II and a shortened form of stem IV, compensatory changes resulted in rates of cleavage equal to or greater than the unaltered ribozyme sequence. Stem III compensatory mutants cleaved faster than the uncompensated mutants although they were not as active as the natural sequence, suggesting additional sequence-dependent requirements within this region. Structure probing of RNA containing the stem II mutations provided an independent confirmation of stem II in the ribozyme. The predictive value of the model was tested by designing two trans-acting ribozymes which were circularly permuted composites of genomic, antigenomic, and unique sequences. The core of these two catalytic RNAs was the same, but they otherwise differed in that, in one of them, a constraining tetraloop sequence was added to stem II. Both ribozymes catalyzed the trans cleavage of a substrate oligoribonucleotide, thus providing additional evidence for stem II and the proposed structure in general.

Self-cleaving sequences present in the genomic and antigenomic RNA of hepatitis delta virus (HDV)[1] may function in vivo to process both the genomic and the antigenomic RNA during rolling-circle replication (Kuo et al., 1988; Sharmeen et al., 1988; Wu et al., 1989). On the basis of the nucleotide sequence flanking the HDV RNA cleavage sites, it was recognized that the HDV self-cleaving structure would represent a motif that is distinct from other self-cleaving RNAs for which secondary structures have been established (Kuo et al., 1988; Sharmeen et al., 1988; Wu et al., 1989). In vitro, the RNA self-cleaves in the presence of Mg^{2+} or other divalent cations, but the observed rate and extent of cleavage vary greatly with both the size of the precursor and the sequences flanking the minimal element (Wu et al., 1989; Rosenstein & Been, 1990; Perrotta & Been, 1990; Belinsky & Dinter-Gottlieb, 1991). For some slow-cleaving precursor sequences, the rate of self-cleavage is greatly stimulated by moderate increases in temperature or the addition of denaturants (Rosenstein & Been, 1990; Belinsky & Dinter-Gottlieb, 1991; Smith & Dinter-Gottlieb, 1991), suggesting that a sizable fraction of the precursor population can fold into long-lived inactive or slow-cleaving structures. In those cases, it is possible that refolding of the RNA to enhance cleavage is facilitated by higher temperatures or the addition of denaturants. However, this explanation remains speculative, and details of the structures, both active and inactive, which are essential to the understanding of the self-cleavage reaction remain to be identified.

Several possible foldings for HDV ribozyme sequences have been presented as potential secondary structures for the self-cleaving sequences from HDV (Wu et al., 1989, 1992; Perrotta & Been, 1991; Rosenstein & Been, 1991; Belinsky & Dinter-Gottlieb, 1991; Branch & Robertson, 1991; Thill et al., 1991). These various models share some common features, but they also differ in important details, such as the boundaries that define the self-cleaving domain within the HDV sequence. In light of the possibility that these sequences may tend to fold into alternative structures, it is important to distinguish between those secondary structures likely to represent the most active self-cleaving form and those foldings which represent interesting but inactive or less active structures.

Although the HDV ribozymes do not share the hammerhead (Hutchins et al., 1986; Forster & Symons et al., 1987) or hairpin–paper clip secondary structures (Hampel et al., 1990; Feldstein et al., 1990), a single structural motif may be shared by the genomic and antigenomic self-cleaving sequences in HDV (Rosenstein & Been, 1991; Perrotta & Been, 1991; Branch & Robertson, 1991). In the version we have proposed (Figure 1a,b), each sequence is folded to include four paired regions, numbered I–IV, 5′ to 3′ from the cleavage site. The 5′ side of stem II is part of the loop defined by stem I; likewise, the 3′ side of stem I is part of the loop defined by stem II. In the structure presented by Branch and Robertson (1991), two pairings largely identical to stems I and IV are proposed. An alternative alignment of nucleotides (nt) forming 2 base pairs at the base of stem IV in that version of the genomic structure is attractive because it allows for a stretch of 3 G's connecting stem I to stem IV to be represented in a similar manner for both the genomic and antigenomic RNAs. That modification has been incorporated into the genomic secondary structure (Figure 1a, compare to inset). In the Branch and Robertson model, additional potential interactions involving bases in the loop generated by stem I (nt positions 8–30 in the genomic and 8–32 in the antigenomic) are not defined, and the 3′ end of the element forming part of stem II (Figure 1a,b) is paired to a sequence 5′ to the cleavage site (nt positions −6 to −3 in the genomic sequence and −5 to −3 in the antigenomic sequence). Therefore, a prediction of this model is that

† Supported by the NIH (GM-40689) and by a North Carolina Biotechnology Center Academic Research Initiation Grant. M.D.B. received salary support from the American Cancer Society (JFRA-233).

* Address correspondence to this author. Telephone: 919-684-2858.

[1] Abbreviations: HDV, hepatitis delta virus; nt, nucleotide(s); PEI, poly(ethyleneimine); TLC, thin-layer chromatography; Tris, tris(hydroxymethyl)aminomethane; EDTA, (ethylenedinitrilo)tetraacetic acid.

0006-2960/92/0431-11843$03.00/0

cleavage activity should show dependence on the sequence of the five to six nt 5′ to the cleavage site; however, that prediction was not tested. The proposed pairing 5′ to the cleavage site is in sharp contrast to our model which, on the basis of results indicating that one nt 5′ to the cleavage site is sufficient for both cis and trans cleavage (Perrotta & Been, 1990, 1992), does not define interactions with sequences 5′ to the cleavage site as part of the ribozyme secondary structure.

Results reported in this paper indicate that mutations in each of the four proposed stems affect the rate constants for self-cleavage in a manner consistent with the proposed structure. The highest rates of self-cleavage were observed in those sequences with the potential to form Watson–Crick-pairing in all four stems. Two small permuted forms of a trans-cleaving ribozyme were generated in which either stem IV or stem II was closed by a stable tetraloop sequence; trans-cleavage activity of these two ribozymes provided additional evidence for the interactions that form stem II and stem IV, and helps define a general form of an active HDV ribozyme.

MATERIALS AND METHODS

Enzymes, Reagents, and Chemicals. T7 RNA polymerase was purified from an overexpressing clone kindly provided by W. Studier (Davanloo et al., 1984). Modified T7 DNA polymerase (Sequenase) was purchased from U.S. Biochemicals (Cleveland, OH). *Eco*RI was provided by Paul Modrich (Duke University). Other enzymes (restriction endonucleases, T4 DNA polymerases, T4 DNA ligase, T4 polynucleotide kinase, and calf intestinal phosphatase), nucleotides, ^{32}P-labeled nucleotides, and chemicals were purchased from commercial sources.

Plasmids. The plasmid pSA1-2 is a synthetic version of the sequence of the antigenomic self-cleaving element inserted downstream of a T7 promoter (Perrotta & Been, 1991). The plasmid pdSIV was made by annealing four oligonucleotides (5′-AATTCGGGTCGGCATGGCATCTCCACCTCC TCGCGGTCCGAC, 5′-TGCCCAGGTCGGACCGCGAG GAGGTGGAGATGCCATGCCGACCCG, 5′-CTGGGCATCTTCGGATGGCTAAGGGAGCA, and 5′-AGCTTGCTCCCTTAGCCATCCGAAGA) and cloning these into pTZ18U that had been cut with *Eco*RI and *Hin*dIII as previously described for the construction of pSA1-2 (Perrotta & Been, 1991). The variants of pSA1-2 and pdSIV were generated by oligonucleotide-directed mutagenesis using a uracil-containing single-stranded form of the plasmid as the template (Kunkel et al., 1987; Vieira & Messing, 1987). The mutagenic oligonucleotides were complementary to the strand of DNA which was of the same sense as the transcript. Trans-cleaving forms of the ribozyme were generated by cloning synthetic double-stranded fragments into pTZ18U. Plasmids with the desired mutation were identified by sequencing miniprep DNA by primer extension with modified T7 DNA polymerase (Tabor & Richardson, 1987) and dideoxynucleotide chain terminators (Sanger et al., 1977). Following a second round of transformation to ensure segregation of the mutated form, plasmid DNA was prepared from overnight cultures by boiling lysis and purified by CsCl equilibrium density centrifugation in the presence of ethidium bromide (Maniatis et al., 1982).

Transcriptions. Plasmid DNA was linearized with *Hin*dIII, extracted with buffered phenol and chloroform and ethanol-precipitated. Transcriptions were carried out in 0.05-mL reactions containing 40 mM Tris-HCl (pH 7.5), 15 mM $MgCl_2$, 5 mM dithiothreitol, 2 mM spermidine, ribonucleoside triphosphates at 1 mM each, 0.05 mCi of [α-^{32}P]CTP, 2.5 μg of linear plasmid DNA, and 300 units of T7 RNA polymerase. Transcription reactions with pdSIV also contained 2 μM oligodeoxynucleotide which was complementary to the sequence in the 5′ portion of the precursor RNA to inhibit self-cleavage during transcription. Incubation was for 60 min at 37 °C, then EDTA was added to 50 mM and formamide to 50% (v/v), and the RNA was fractionated by electrophoresis on a 6% (w/v) polyacrylamide gel containing 7 M urea. RNA was located by autoradiography, excised, eluted overnight at 4 °C [in 10 mM EDTA and 0.1% (w/v) sodium dodecyl sulfate], and recovered by ethanol precipitation. In the preparation of trans-acting ribozymes, the transcription reaction was scaled up to 0.5 mL, the label was omitted, and the RNA was located by UV-shadowing following electrophoresis.

Self-Cleavage Reactions. Radiolabeled precursor RNA generated by in vitro transcription was separated from the cleaved material by gel electrophoresis under denaturing conditions in the presence of EDTA to prevent additional self-cleavage. Precursor RNA was preincubated at 37 °C for 5 min in the cleavage cocktail minus Mg^{2+}, and the cleavage reactions were initiated by the addition of $MgCl_2$ (prewarmed to 37 °C); final conditions were 40 mM Tris-HCl (pH 8.0), 1 mM EDTA, 11 mM $MgCl_2$, and approximately 5–50 nM RNA. For reactions that contained 10 M formamide, the formamide was included in the preincubation. For time points, 5-μL aliquots were removed and quenched by mixing with 5–10 μL of formamide/dye mix containing 25–50 mM EDTA. Precursor and product were separated by denaturing gel electrophoresis [6% polyacrylamide (bis(acrylamide):acrylamide ratio of 1:29) gels containing 7 M urea, 0.05 M Tris–borate, pH 8.3, and 0.5 mM EDTA]. The precursor and 3′-cleavage product were located by autoradiography, excised, and quantified by counting Cherenkov scintillation. The 5′ product migrates off these gels and was not recovered. The fraction cleaved (F) was calculated as $[cpm^{product}/(cpm^{precursor} + cpm^{product})]/N$, where $cpm^{precursor}$ and $cpm^{product}$ have been corrected for background counts and N is the fraction of label present in the 3′ fragment (N = 0.95–0.97 for the precursors used in this study). The first-order rate constant (k), and end point (EP), and the standard errors (SE) were obtained from nonlinear least-square fits of the data to the equation $F = EP(1 - e^{-kt})$, using Systat software. The half-lives ($t_{1/2}$) for precursors reported in the text were calculated from $t_{1/2} = 0.693/k$. For the faster cleaving sequences, the end point was also estimated from time points taken at 5–60 min [$(10–200)t_{1/2}$]. At these extended time points, the experimentally determined end point often exceeded the calculated value (which ranged from 0.49 to 0.89) by 5–10%, suggesting that there may be a slow-cleaving precursor population in those preparations. However, to simplify the presentation of the data, all reactions were analyzed as though they contained a single major species that cleaved with simple first-order kinetics, and both the end point and the first-order rate constant are given for the fast phase of the reaction with each precursor.

Trans-Cleavage Reactions. Substrate, DHS4 (rC^GGGUCGG), was chemically synthesized (at U.S. Biochemicals) and gel-purified (Perrotta & Been, 1992). For multiple turnover experiments, trace amounts of 5′-^{32}P end-labeled DHS4 were mixed with known quantities of unlabeled DHS4. Substrate and enzyme were preincubated separately in 40 mM Tris-HCl (pH 8 at 25 °C), 1 mM EDTA, and 11 mM $MgCl_2$ for 2 min at 37 °C and then mixed to start the reaction. Variations in the time and temperature of the preincubation were not seen to have an effect on the subsequent

reactions. Samples (2 μL) were removed at the determined times and fractionated by TLC which separates the labeled nucleoside 5′-phosphate 2′,3-cyclic phosphate from the uncleaved substrate (Perrotta & Been, 1992). Radioactive spots were located by autoradiography, excised, and counted. For single-turnover experiments, trace amounts of labeled DHS4 (<1 nM) were used with increasing concentrations of CDC200 or PDC7 RNA. At least three time points were taken for each enzyme concentration; these were fractionated by TLC and quantified as described above. Pseudo-first-order rate constants obtained for each enzyme concentration were fit to the equation given in the text to obtain a rate constant (k) and the Michaelis constant (K_M).

Structure Probing with Nuclease V1. Reaction conditions for nuclease V1 digestion were described previously (Rosenstein & Been, 1991). Briefly, 5′ end-labeled 3′-cleavage product RNA was preincubated at 37 °C in V1 cocktail containing 0 or 5 M urea, and the nuclease was added. Reactions were terminated by adding formamide/EDTA/dye mix and putting them on crushed dry ice.

RESULTS

Characteristics of Self-Cleavage of the Antigenomic Sequence SA1-2. A synthetic version of the antigenomic self-cleaving element SA1-2 (Figure 1c) has been described previously (Perrotta & Been, 1991). Under conditions used for transcription, 45–55% of the RNA is cleaved during in vitro transcription; however, with chelation of the Mg^{2+}, the purified precursor is stable and does not cleave until Mg^{2+} is added again to initate the reaction. With different preparations of purified SA1-2 precursor, approximately 55–70% of the RNA will cleave. For a given preparation of RNA, the proportion that cleaved was not increased by repeated cycles of heating and cooling (95 and 37 °C), and less than 5% of the reisolated uncleaved material (after 30 min at 37 °C) cleaved when tested again (data not shown). This suggested that, for the SA1-2 precursor, the uncleaved portion that remained is either an exceedingly stable alternative conformer of the RNA or, more likely, contaminating noncleavable sequences that copurified with the precursor. However, with the other sequences used in this study, the extent of cleavage varied, both during transcription and in the subsequent reactions with purified precursors. Also, with some precursor sequences, the extent of cleavage increased in 10 M formamide, suggesting that, in those cases, noncleaving conformers do contribute to the observed end points.

At 37 °C in 10 mM Mg^{2+}, nearly half of the SA1-2 precursor had cleaved by the first time point at 8 s (Figure 2a). The reaction was essentially complete after 1 min in that the extent of cleavage at 5, 10, and 30 min was not significantly greater than that at 1 min (data not shown). The data from independent time courses using four different preparations of SA1-2 precursor were quantified and plotted (Figure 3a); the solid line was generated using a first-order rate constant, k, of 4.7 min^{-1} ($t_{1/2}$ of about 9 s) with an end point of 0.65 (Table I). The addition of 10 M formamide to the reaction appeared to give a small increase in the rate constant (~2-fold, k = 10 min^{-1}) without greatly increasing the end point (EP = 0.70) (Figure 3b). Due to uncertainties in mixing times, temperature fluctuations, and quenching times, rate constants this fast are only approximate; however, the 2-fold difference in rate constants for SA1-2 precursor measured with and without formamide is always reproducible. The effect on the kinetics of cleavage of each mutation or combinations of mutations in stems I, II, and III will be compared to results with SA1-2 (Table I).

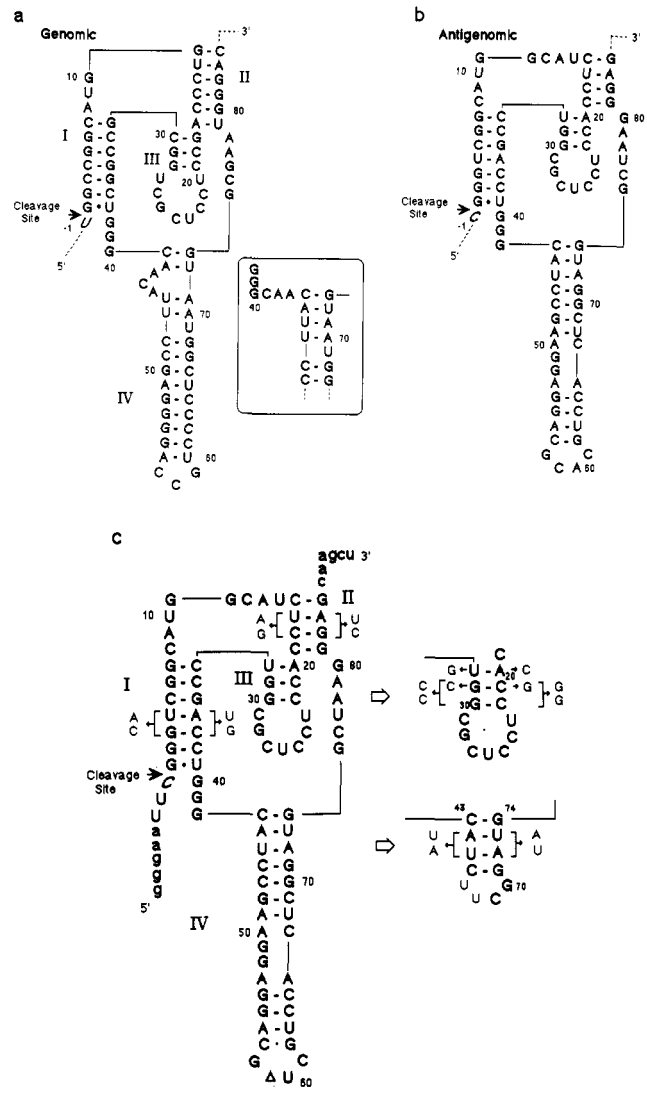

FIGURE 1: Proposed HDV ribozyme secondary structures. (a and b) Secondary structures for the genomic and antigenomic self-cleaving sequences of HDV ribozymes. Arrows indicate the sites of cleavage, and numbering is from the site of cleavage. An alternative alignment at the base of stem IV in the genomic sequence (see text) is illustrated in the inset. (c) Mutations made in SA1-2, a synthetic version of the antigenomic sequence, used in this study. The SA1-2 sequence differs from the wild-type antigenomic sequence in the loop of stem IV and in vector-derived flanking sequences which are shown in lower case letters. The entire sequence of the SA1-2/*Hin*dIII runoff is shown. The mutations in stems I and II are the same as previously described (Perrotta & Been, 1991), and the changes made to stem III and the deleted form of stem IV are shown to the right.

Mutations in Stems I and II. In both the genomic and antigenomic structures, stems I and II define the boundaries of the self-cleaving sequences. Stem I, a 7 base pair duplex adjacent to the site of cleavage, contributes to substrate selection in a trans reaction (Perrotta & Been, 1992). For the self-cleavage reaction, the introduction of G3c and U4a mismatches (G to C at position 3, and U to A at position 4) in the 5′ side of stem I (SI5′, Figure 1c) or A36u and C37g in the 3′ side (SI3′, Figure 1c) substantially reduced the rate of cleavage (Figure 2b). After 1 min, where the cleavage reaction of SA1-2 is complete, less than 2% of the SI5′ or SI3′ precursor has cleaved. After 30 min, approximately 10% has cleaved. For SI5′, the rate constant for cleavage was down about 400-fold (k = 0.012), and for SI3′, the rate constant was down 60-fold (k = 0.08) (Table I).

The potential for base-pairing in SI is restored when both sets of base changes are combined to generate SI5′3′. The

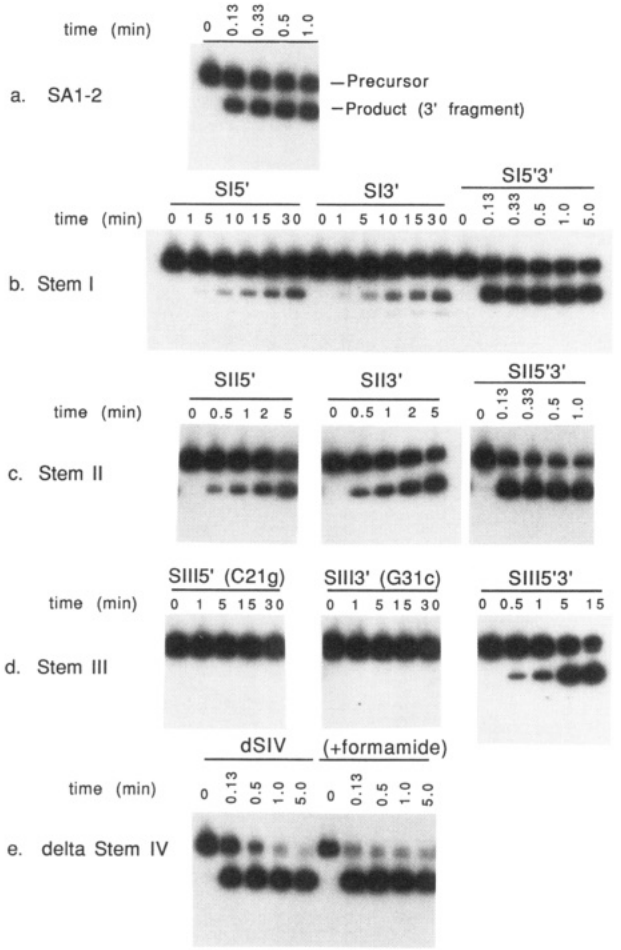

FIGURE 2: Self-cleavage reactions. All reactions were as described under Materials and Methods and were carried out in the absence of denaturants except as indicated. In each case, the upper band is the precursor, and the lower band is the 3′-cleavage product. Examples of autoradiograms are shown from time courses for (a) SA1-2, (b) stem I mutants, (c) stem II mutants, (d) stem III mutants [C21g, G31c, and the double mutant (C21g:G31c], and (e) dSIV cleaved in the absence and presence of formamide.

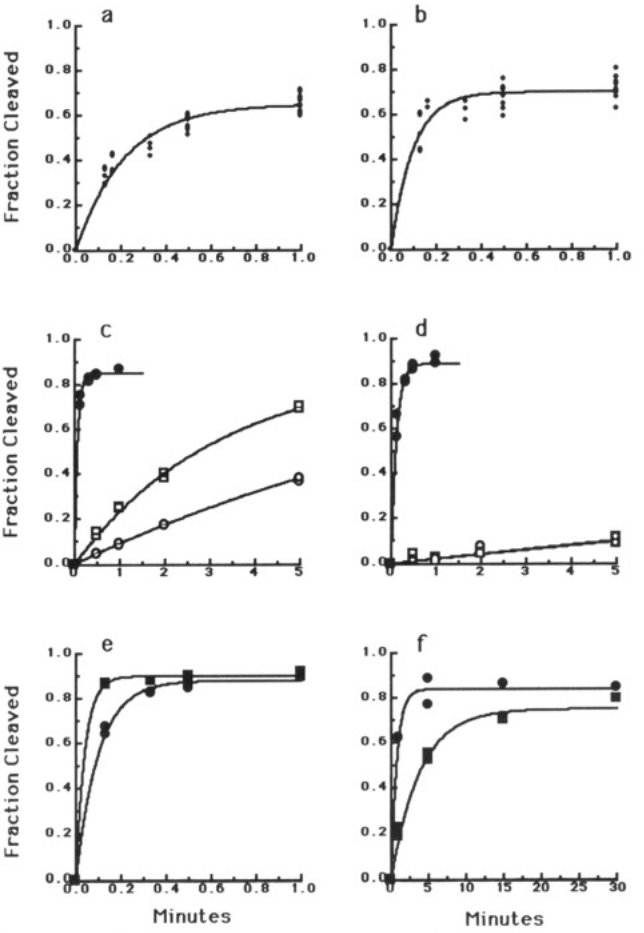

FIGURE 3: Kinetics of cleavage. Data from independent time courses are superimposed on graphs of theoretical curves generated with the data in Table I. (a) SA1-2. (b) SA1-2 in 10 M formamide. (c) Stem II mutants: SII5′ (open circles); SII3′ (open squares); SII5′3′ (closed circles). (d) Stem II mutants in 10 M formamide; the symbols are the same as in graph c. (e) Stem IV mutants: dSIV (circles); dSIV5′3′ (squares). (f) Stem IV mutants: dSIV5′ (squares); dSIV3′ (circles). For all graphs, the fraction cleaved is plotted as a function of time in minutes; note that individual time courses varied from 1 to 30 min.

compensatory base changes restored the higher rate of cleavage (Figure 2b). The $t_{1/2}$ is about 3 s (k = 14 min^{-1}, Table I). At this rate, the reaction would have gone through 2 half-lives by the first time point (8 s). Therefore, while there may be a systematic error in the estimate of the rate constant, the rate constant for the compensatory mutant is reproducible and very close to that for the SA1-2, if not higher.

Cleavage of SI3′ generated a small amount of a second, faster running product (Figure 2b). The identity of this band has not be determined, but it could be due to cleavage between C5 and G6, 5 nt 3′ to the original cleavage site. The sequence at this secondary cleavage site would form an acceptable stem I in a precursor containing the SI3′ mutation (Figure 1b): it would contain one U-G base pair but would otherwise be identical to stem I in the SI5′3′ double mutant.

Stem II is a short pairing involving sequences at the 3′ end of the self-cleaving domain and sequences in the loop defined by stem I. We have previously shown that the requirement for base-pairing in stem II is most obvious when the cleavage reaction is carried out in 10 M formamide (Perrotta & Been, 1991). It was less apparent from these data that disruption of base-pairing in stem II (SII5′ and SII3′, Figure 1c) also affected cleavage in the absence of denaturants. However, an examination of the kinetics of the reaction in both the absence and presence of denaturant showed that the effects of the mutations are general (Figures 2c and 3c,d). In the absence of denaturants, the rate constant for cleavage of SII5′ was down almost 50-fold (k = 0.10 min^{-1}) and that of SII3′ was down 15-fold (k = 0.31 min^{-1}) relative to SA1-2. In the presence of formamide, the differences were greater, with the rate constants down 400-fold for both SII5′ and SII3′ (Table I). The combination of mutations, which restored base-pairing in stem II, restored the higher rate constant for self-cleavage in both the absence (k = 15 min^{-1}) and presence of formamide (k = 8 min^{-1}). Therefore, formamide exaggerated the differences between those precursors which are capable of base-pairing in stem II and those which are not. A similar effect of formamide had been seen in stem I (Table I).

A restriction endonuclease site (*Dde*I) makes it possible to generate a precursor which ends after position 79, one nucleotide short of the 3′ side of stem II. SA1-2/*Dde*I precursor is deleted of sequences involved in the formation of the 3′ side of stem II. It cleaves, but with a substantially lower rate constant (k = 0.01 min^{-1}) than the *Hin*dIII runoff of SA1-2 (Table I). The addition of formamide to the reaction further reduced the rate of cleavage, but the data were not quantified. A *Dde*I runoff of the SII5′ mutant cleaved with a rate constant (k = 0.22 min^{-1}) close to the *Hin*dIII runoffs of the SII5′ (0.10 min^{-1}) and SII3′ (0.31 min^{-1}) mutants.

Table I: Rate Constants for Cleavage in the Absence and Presence of Denaturant[a]

precursor RNA	k (min^{-1})	SE	EP	% wt k	k^f (min^{-1})	% wt k^f
SA1-2 (wt)	4.7	0.3	0.65	100	10.4	100
SA1-2/*Dde*I	0.010	0.003	0.57	0.21	–	–
SI5′ (G3c,U4a)	0.012	0.004	0.41	0.26	<0.001	<0.01
SI3′ (A36u,C37g)	0.08	0.01	0.12	1.7	<0.001	<0.01
SI5′3′	14	2	0.49	300	10	96
SII5′ (U17a,C18g)	0.10	0.02	0.97	2.1	0.023	0.22
SII3′ (G81c,A82u)	0.31	0.03	0.88	6.6	0.024	0.23
SII5′3′	15	1	0.85	320	8.4	81
SII5′/*Dde*I	0.22	0.02	0.77	4.7	–	–
SIII5′ (A20c)	0.14	0.07	0.74	3.0	[0.012]	0.12
SIII3′ (U32g)	0.25	0.06	0.71	5.3	[0.007]	0.067
SIII5′3′	1.0	0.1	0.75	21	0.59	5.7
SIII5′ (C21g)	<0.001			<0.02	<0.001	<0.01
SIII3′ (G31c)	<0.001			<0.02	<0.001	<0.01
SIII5′3′	0.22	0.03	0.89	4.7	0.05	0.48
SIII5′ (C21g,C22g)	<0.001			<0.02	<0.001	<0.01
SIII3′ (G30c,G31c)	<0.001			<0.02	<0.001	<0.01
SIII5′3′	1.4	0.2	0.68	30	0.08	0.77
dSIV	11	1	0.83	230	15	144
dSIV5′ (A44u,U45a)	0.26	0.04	0.75	2.4[b]	0.14	1.3[b]
dSIV3′ (A72u,U73a)	1.3	0.2	0.84	12[b]	0.12	1.2[b]
dSIV5′3′	23	4	0.84	200[b]	25	170[b]
dSIVB	0.059	0.003	0.79	1.2	–	–

[a] All runoffs, except for those denoted by /*Dde*I, were *Hin*dIII runoffs. For reactions carried out in the absence of formamide, rate constants (k), error estimates (SE), and the end point (EP) of the reaction were obtained from nonlinear least-square fits to the equation given under Materials and Methods. For reactions done in the presence of 10 M formamide, only the rate constant is given (k^f). Values given in brackets are estimated from slopes of first-order plots without correcting for end points and therefore are lower limits. Values <0.001 were given to variants with essentially no cleavage activity. For each set of mutants, the nomenclature refers to mutations in the 5′ side of the stem, the 3′ side of the stem, or the compensatory combination of those mutations. Mutations were generated in the SA1-2 (antigenomic) sequence except for the stem IV mutations, which were made in a shortened form of stem IV (dSIV). Dashes indicate reduced cleavage activity in the presence of formamide that was not quantified. [b] Rate constants for the dSIV mutants were compared to dSIV not to SA1-2.

Evidence for Structural Changes in RNA Containing the Stem II Mutations. While a structural basis for the effect of the stem II mutations is inferred from the effects on the kinetics of cleavage, it is also possible to probe structural changes directly. The sequence 3′ of the cleavage site (in the form of the 3′-cleavage product), which contains all essential components of the ribozyme except for a nucleotide 5′ to the cleavage site, has been probed with nucleases (Rosenstein & Been, 1991). The digestion patterns were generally consistent with the proposed models. 3′-Product RNA isolated from cleavage reactions with SII5′, SII3′, and SII5′3′ precursors was 5′ end-labeled and probed with cobra venom (V1) nuclease; the digestion patterns were compared to similar digestions of SA1-2 (WT) 3′-cleavage product (Figure 4). V1 nuclease cuts preferentially in helical or stacked regions with little sequence preference (Lowman & Draper, 1986; Ehresmann et al., 1987). In the SA1-2 sequence, major cut sites were observed in the 5′ and 3′ sides of stem I (U4, C5, and G35) and the 5′ side of stem II (U17 and C18) (lanes 5, 6, 7, 14, and 15). When either side of stem II was mutated (5′, lanes 8, 9, 16, and 17; or 3′, lanes 10, 11, 18, and 19) the cuts at positions 17 and 18 largely disappeared. In SII5′ and SII3′, the pattern of cutting in the region between positions 16 and 26 changed dramatically, although cuts in stem I were not affected. With the compensatory change, SII5′3′ was again cut at positions 17 and 18, and the overall pattern appeared more similar to the SA1-2 RNA than to either SII5′ or SII3′.

More obvious alterations in cutting patterns for the different variants were seen in the presence of 5 M urea than in its absence (Figure 4, compare right and left sides of the gel). Urea, like formamide, will enhance cleavage rates for the wild-type HDV ribozymes (Rosenstein & Been, 1990, unpublished results). Urea was used previously in structure probing studies of the HDV ribozyme where, in the presence of 2–10 mM Mg^{2+}, it "enhanced" cutting patterns (Rosenstein & Been, 1991). For the stem II variants, the addition of urea did enhance V1 cutting in the stem III and stem loop III sequences. Because nuclease V1 will cut in stacked helical sequences which need not be duplex (Lowman & Draper, 1986), these results do not necessarily imply that the stem loop III sequence assumes an alternative base-paired structure with the SII mutants; it could be that disruption of base-pairing in stem II makes an otherwise good substrate (stacked loop nucleotides) for nuclease V1 more accessible to that nuclease. The addition of urea, by further destabilizing residual stem II or other interactions, could increase this accessibility. If the sequence of stem loop III actually adopted alternative structures, a loop in SA1-2 and SII5′3′, but a duplex in SII5′ and SII3′, the results would suggest that the alternative structure would be more stable in the presence of denaturant (Figure 4 and data not shown).

Stem III. Stem III, as drawn, contains 3 base pairs and is closed by a loop of 8 nt in the genomic and 7 nt in the antigenomic sequence. Several changes and compensatory changes were made in the stem III sequence; the effects were variable, and some were dramatic. Disruption of the covariant positions (A20c or U32g) resulted in a 20–30-fold decrease in the rate constant for cleavage, while the compensatory combination resulted in a 4–7-fold enhancement over the single mutants. The rate constant for cleavage in the compensatory mutant was down 5-fold from SA1-2 (Table I). In contrast, no cleavage was detected after 30 min with precursors containing a C21g (5′ side) or a G31c (3′ side) mutation (Figure 2). We estimate that the rate constant for cleavage was down at least 4 orders of magnitude. The compensatory mutant, C21g:G31c, restored cleavage to a measurable level (k = 0.22 min^{-1}); it was down 20-fold relative to SA1-2, but up more than 200-fold relative to the single mutants. In contrast to the compensatory mutations in stems I and II, the addition of formamide to the reaction with the C21g:G31c compensatory change resulted in a further reduction in the rate constant (k = 0.05 min^{-1}).

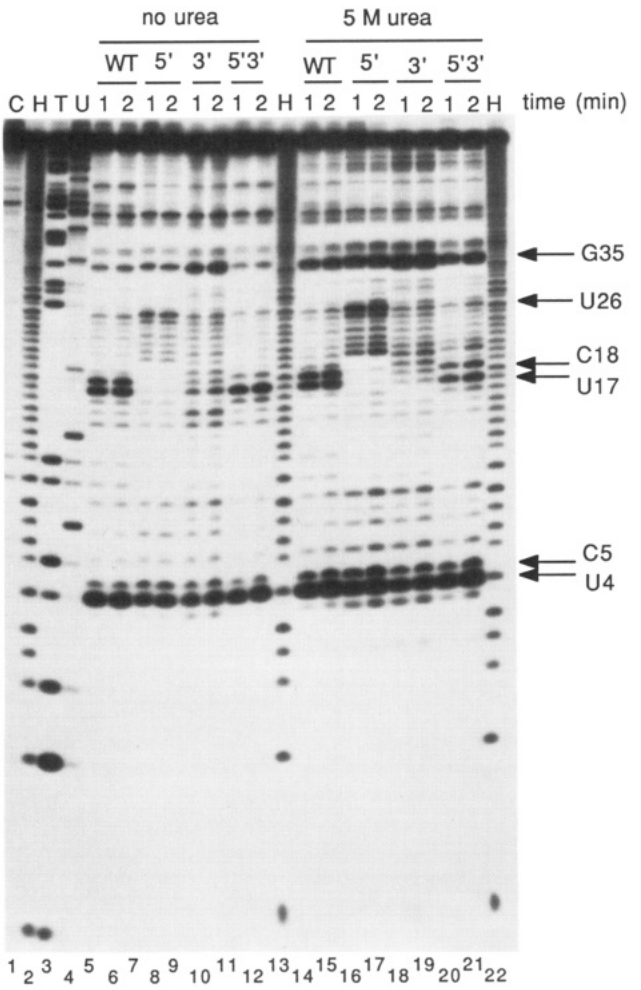

FIGURE 4: Nuclease V1 probing of stem II mutants. Reactions contained 0.01 unit/μL V1 and either no urea (lanes 5–12) or 5 M urea (lanes 14–21) and were incubated at 37 °C for 1 and 2 min. The RNAs used were (WT) SA1-2, (5′) SII5′, (3′) SII3′, and (5′3′) SII5′3′. Lanes 1–4 contained markers generated using SA1-2 RNA: C, untreated controls; H, alkaline hydrolysis; T, RNase T1; U, RNase U2. Samples were fractionated by electrophoresis on a 20% polyacrylamide gel containing 7 M urea, and an autoradiogram is shown. Note that V1 products contain a 3′-hydroxyl group and thus show a reduced mobility relative to the 3′(2′)-phosphate group containing markers.

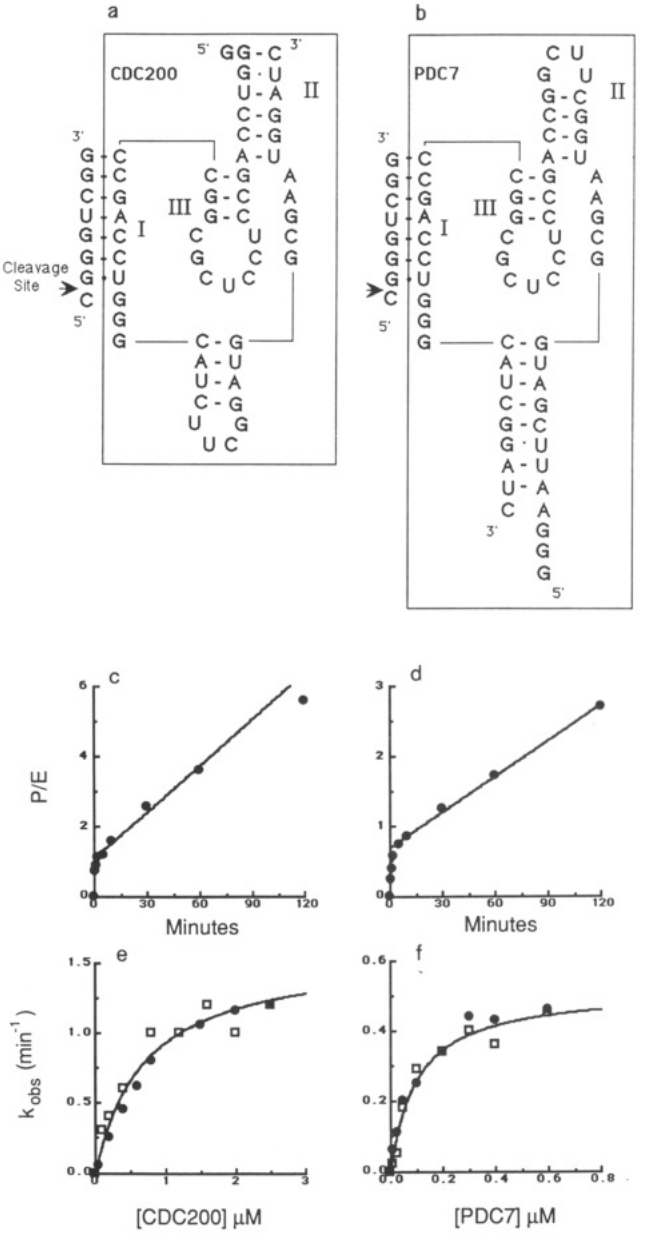

FIGURE 5: Circularly-permuted trans-cleaving composite ribozymes. (a and b) Sequences and proposed secondary structures of CDC200 and PDC7 RNAs. Each ribozyme is shown base-paired with the substrate oligoribonucleotide. (c and d) Cleavage reactions with excess substrate using CDC200 and PDC7, respectively. Moles of product generated per mole of enzyme (P/E) as a function of time is plotted. The lines are fit to the initial portion of the steady-state region of the time course and have intercepts of 1.1 ± 0.1 and 0.7 ± 0.1 P/E and slopes of 0.044 ± 0.004 and 0.017 ± 0.002 min^{-1} for CDC200 (c) and PDC7 (d), respectively. (e and f) Single-turnover kinetics. Different symbols represent two independent sets of rate determinations; solid lines are theoretical curves generated with the kinetic constants given in the text.

Additional mutations in stem III, C to G changes at positions 21 and 22, and G to C changes at positions 30 and 31, also resulted in dramatic loss of activity, but the compensatory combination restored activity; the rate constant for cleavage was at least 10^3-fold higher than in the uncompensated mutants (Table I). Although the compensatory mutant had a rate constant for cleavage (1.4 min^{-1}) close to that of SA1-2 in the absence of denaturant, in the presence of 10 M formamide the rate constant was down 10^2-fold.

Stem IV. Before making specific base changes in stem IV to test base-pairing possibilities, we made two deleted forms. dSIV (Figure 1c) contains a deletion of all but 4 base pairs of stem IV; this shorter version is closed with a tetraloop sequence (UUCG). dSIVB contains a deletion of essentially all of stem IV. In its place, C43 is joined to G74, thus replacing the stem with a dinucleotide. dSIV cleaved rapidly and to near-completion (k = 11 min^{-1}, EP = 0.88) (Figures 2e and 3e) while dSIVB cleaved about 100-fold slower than SA1-2 (k = 0.06 min^{-1}). dSIVB was not examined further.

Using the dSIV sequence, changes were made in the 5′ and 3′ sides of the truncated stem IV (Figure 1b). Moderate decreases in rate constants were observed for dSIV5′ and dSIV3′ (Figure 3f) (k = 0.26 and 1.3 min^{-1}, respectively). However, the compensatory mutant, dSIV5′3′, cleaved as fast or faster (k = 25 min^{-1}) than did dSIV (Figure 3e). We conclude that base-pairing within the sequence forming stem IV is required for efficient cleavage activity.

Circularly-Permuted Composite Trans-Acting Delta Ribozymes. The information gained from the above analysis has been applied to the design of two novel trans-acting ribozymes with the general HDV motif (Figure 5). Each ribozyme contains short regions from the antigenomic sequence [the 3′ side of stem I, the sequence joining stems I and IV (JI/IV), part of stem IV, and stem loop III] and the genomic

sequences [stem III, the region joining stems IV and II (JIV/II), and part of stem II]. The only differences between the two RNAs reside in the sequences making up stem II and stem IV. In CDC200, the sequence begins and ends in stem II, and stem IV is closed with a tetraloop. In PDC7, the sequence beings and ends in stem IV while stem II is closed with a tetraloop. Stem I is formed through an intermolecular association with a substrate oligonucleotide as previously described (Perrotta & Been, 1992).

Both forms of the trans-acting ribozyme were active. When the substrate 8-mer is 5′ end-labeled with ^{32}P, cleavage releases a cytidine 2′,3′-cyclic 5′-[^{32}P]-diphosphate which can be followed by thin-layer chromatography (Perrotta & Been, 1992). At 37 °C in 10 mM Mg^{2+}, with substrate in 10-fold excess, there is a burst of product release followed by a slower rate of product formation (Figure 5c,d). The burst size is consistent with approximately 1.1 (±0.1) mol of product per mole of CDC200 and 0.7 (±0.1) mol of product per mole of PDC7. This suggests that the first binding event results in rapid cleavage but then there is a change in the rate-limiting step to a slow step subsequent to cleavage, resulting in slow turnover. The burst size near unity indicates that most of the enzyme is active. Slow turnover was seen with an earlier form of the trans-acting ribozyme, ADC1 (Perrotta & Been, 1992), and slow product release was suggested as one possible cause of the low turnover.

For trans cleavage, the rate of product formation during the burst is the relevant parameter to use for comparison to the self-cleavage reaction because self-cleavage is a single-turnover reaction. The pre-steady-state kinetics of the trans reaction were therefore examined. Using trace amounts of labeled substrate, pseudo-first-order rate constants for cleavage (k_{obs}) were determined with increasing enzyme concentrations (Figure 5e,f). In each case, the rate of cleavage plateaus at high enzyme concentrations, consistent with a change in the rate-limiting step or saturation of the substrate. The data were fit to the equation $k_{obs} = k[E]/(K_M + [E])$ using a nonlinear least-squares curve-fitting program, where k is the rate constant for single-turnover at saturating [E] and K_M is the Michaelis constant representing the enzyme concentration giving half-maximal rate of cleavage. For CDC200, $k = 1.5 \pm 0.1$ min^{-1} and $K_M = 0.7 \pm 0.1$ μM ($k/K_M = 2 \times 10^6$ M^{-1} min^{-1}). For PDC7, $k = 0.52 \pm 0.05$ min^{-1} and $K_M = 0.10 \pm 0.02$ μM ($k/K_M = 5 \times 10^6$ M^{-1} min^{-1}). Therefore, the single-turnover rate constant is 3–10-fold lower than the first-order rate constant for the self-cleaving form of the SA1-2 precursor, suggesting that the rate-limiting step for cleavage could differ for these cis and trans forms of the reaction. The second-order rate constants (k/K_M) are within a factor of 3 of each other but are less than the 10^7–10^8 M^{-1} min^{-1} values obtained for association of oligonucleotides to form duplex (Nelson & Tinoco, 1982) and the binding of substrate oligonucleotide by the *Tetrahymena* ribozyme (Herschlag & Cech, 1990).

DISCUSSION

Mutations in Duplex Regions Affect the Rate Constants of Self-Cleavage. In every one of the four proposed paired regions, mutations that disrupted base-pairing resulted in decreased activity whereas mutations in combinations that regenerated the hypothesized pairings also restored a level of activity that was greater than either noncompensated mutant. If those sequences were not base-paired as is proposed in the model, the combination of mutations would be expected to be no more active, or possibly less active, than either mutation by itself. Therefore, the results provide strong support for the proposed model.

How might the mutations affect the experimentally measured rate constant for cleavage? In a simple kinetic scheme for the self-cleavage reaction where the reaction is initiated with the addition of $MgCl_2$, there may be a preequilibrium between inactive (R_i) and active (R_a) structures of the RNA precursor (step 1). As suggested by end points less than 100%, some of the RNA may also partition into a completely inactive form ("R_{dead}") for which essentially no further activity is observed. Cleavage chemistry occurs in a second step with R_a to generate the two products. Although the products may dissociate in a third discrete step, our assay does not distinguish between the products of cleavage that have and have not dissociated. True reversal of the cleavage reaction has not yet been demonstrated, so, presumably, under the conditions being used, the equilibrium for cleavage or dissociation or both would be far toward product formation and we can combine those steps in a simplified scheme (Scheme I).

Scheme I

$$R_i \underset{k_{-1}}{\overset{k_1}{\leftrightarrow}} R_a \xrightarrow{k_2} P1 + P2$$

The results from the mutagenesis and kinetic studies indicate that disruptions of the paired sequences had to have either (i) decreased the rate constant for a rate-limiting step, (ii) decreased the rate constant of another step so that it becomes rate-limiting, or (iii) decreased the concentration of active precursor in the preequilibrium ($K_{eq} = k_1/k_{-1}$). If the preequilibrium is rapid relative to subsequent steps ($k_{-1} \gg k_2$), then changes either to the preequilibrium constant (K_{eq}) or to k_2 will be seen as alterations in the observed first-order rate constant because $k_{obsd} = k_2[R_a]/([R_a] + [R_i]) = k_2/(1 + 1/K_{eq})$. Thus, while k_2 would be rate-limiting, k_{obsd} would be less than k_2 except when K_{eq} is large and most of the precursor is in the active conformation. Alternatively, if the preequilibrium is not rapid ($k_2 \gg k_{-1}$), then either k_1 or k_2 or a combination of both could be rate-limiting. Mutations in duplex regions could have affected the relative stability of alternative structures in the RNA, thus altering either the equilibrium constant or the rate constants defining the equilibrium for cleavable and noncleavable conformations of the RNA. Increasing K_{eq} (or k_1 and k_{-1}) may be an explanation for why some of the compensatory changes resulted in moderate increases in the rate constant for cleavage relative to the SA1-2 precursor; it could also explain why denaturants (formamide or urea) can enhance cleavage of some precursors. However, it is also possible that some mutations will affect k_{obsd} by altering the rate constants for steps making up k_2 (for example, chemistry, or other slow conformation changes prior to chemistry, or in the case where the equilibrium constant for chemistry is unfavorable, product dissociation). Clearly, further characterization of the reactions for each mutant would be necessary to assign an effect of the mutations to changes in a particular constant in the kinetic scheme. Nevertheless, in the simplest model for cleavage, the proposed structure would be the most active form of the ribozyme, and in a complex model, each secondary structural element would be required for one or more folding intermediates.

Stem I. Changes in either side of stem I, which would destabilize this pairing, were found to dramatically reduce the rates of cleavage (50–400-fold). With the positions tested,

the evidence suggests that altering the sequence while maintaining Watson–Crick-pairing had only minimal effects on the rate of cleavage. The effect of compensatory changes in stem I was to restore the rate for cleavage to the original level (a slight, 2–3-fold, reproducible increase in the rate of cleavage was actually measured). The predicted stability of stem I in SI5′3′ relative to SA1-2 is essentially the same ($\Delta\Delta G°$ = 0.5 kcal/mol; Frier et al., 1986). If the 2–3-fold increase in rate was real, it would suggest that within stem I not all base pairs are equal, and we would predict that some base pair combinations could also cause a slight decrease in the rate of cleavage.

Stem II. Mutations that would be expected to destabilize stem II had a less dramatic effect than those in stem I. Even so, in $MgCl_2$ at 37 °C, without denaturant, cleavage was down 10–50-fold for the SII5′ and SII3′ mutants. The compensatory changes made to stem II in SII5′3′ would again be predicted not to alter the stability of the helix ($\Delta\Delta G°$ = 0 kcal/mol; Frier et al., 1986), yet, as with stem I, the compensatory combination resulted in a small (3-fold) increase in the rate of cleavage relative to SA1-2, indicating that at least the original rate of cleavage was restored.

The effect of disruptive and compensatory mutations in stem II on ribozyme structure was also examined directly in a structure probing experiment. Mutations in either side of stem II altered the pattern of V1 cutting in the 5′ sides of stem II and stem loop III. Alterations in the nuclease digestion patterns appear to be mostly localized to a 10-nucleotide region comprising positions 17–26, even when the mutations are made at positions 82 and 83 (compare WT to SII3′, and SII5′ to SII5′3′); this result provides direct physical evidence for the stem II interaction. Combined with the kinetic studies, it validates the use of mutagenesis and functional assays to study the HDV ribozyme structure.

We previously had shown that stem II is a feature which serves to facilitate cleavage under conditions that would otherwise lessen the overall stability of the RNA structure, such as when denaturants are added to the reaction (Perrotta & Been, 1990, 1991). In those reports, it was less obvious that the mutations affected cleavage in the absence of denaturants because the differences in rates of cleavage were not apparent with the single time points shown. In this study, we showed that the denaturant (10 M formamide) did exaggerate the differences in the relative rates; the SII5′ and 3′ mutants were down 450-fold relative to the SA1-2 precursor. However, the kinetics indicate that stem II is an important feature for optimal self-cleavage in both the absence and presence of denaturants.

A deletion at the 3′ end provides additional evidence for stem II. A *Dde*I runoff of the antigenomic ribozyme can generate a self-cleaving precursor which contains only 79 nt 3′ to the cleavage site (Been & Perrotta, 1991; Smith & Dinter-Gottlieb, 1991). In our assays, this deletion resulted in a 50–500-fold decrease in the rate constant (SII5′/*Dde*I relative to SII5′3′/*Hin*dIII, and SA1-2/*Dde*I relative to SA1-2/*Hin*dIII, respectively). Smith and Dinter-Gottlieb (1991) observed a decreased extent of cleavage after 5 min at 37 °C with a *Dde*I runoff relative to longer versions of an antigenomic ribozyme precursor. They also observed decreased activity in denaturant with the *Dde*I runoff, but attributed it to loss of a 17-nt stem and loop structure which spans the 3′ boundary of the ribozyme domain which we have defined as a minimal sequence requirement (Perrotta & Been, 1991). That particular stem and loop would not form in the SA1-2 and variant sequences that we have used, and as such, their results are consistent with our model, but their model would not predict our results.

Stem III. In addition to the current mutagenesis and previous structure probing data (Rosenstein & Been, 1991), stem III has an identical location relative to stems I and II in both the genomic and antigenomic sequences, and contains a covariant base pair (an A-U in the antigenomic is replaced by a G-C in the genomic). As drawn, stem III could form a coaxial stack with either stem I or stem II, although it may well stack with neither. Since the 3′ side of stem II can be deleted with only partial loss of activity, one might predict that given the choice of one stacking possibility or the other it must then stack on stem I. We would also consider an additional interpretation of the same data; that is, stem II contributes to the stability of the cleavable structure because, through coaxial stacking, it could stabilize stem loop III and maintain it in the most favorable position and configuration for cleavage.

Several of the mutations in stem III that disrupt the potential for base-pairing had large effects on the rates of cleavage, and the compensatory mutations in stem III did not restore full cleavage activity. Despite this partial restoration in activity, the increase over the uncompensated mutation was substantial; in one set of mutants, it was up perhaps 10^3-fold (C21g,C22g: G30c,G31c) (Table I). A general negative effect of altering the base pairs in stem III could have several explanations. It is possible that base triplets or other tertiary interactions involving the duplex would place constraints on the sequence of stem III. In that regard, it is interesting that folding programs which have been used to generate lowest free energy secondary structures, but do not yet incorporate contributions from tertiary interactions, did not predict stem III (Wu et al., 1989; Thill et al., 1991). Another possibility is that stem loop III is part of the catalytic core and alterations to the stem perturb the loop structure, thereby affecting the rate of cleavage by altering the active-site structure.

An interesting effect with deletions in the stem loop III region of the genomic ribozyme has been reported by Suh et al. (1992). In a small, apparently very active, form of the genomic ribozyme (HDV88), a deletion that includes the 5′ side of stem II and all of stem and stem loop III resulted in total loss of self-cleavage activity. However, in a less active form of a precursor (HDV133), containing an additional 45 nt of flanking sequences not normally required for cleavage activity (Perrotta & Been, 1991), the same deletion resulted in substantial but partial loss of activity. They reported 45–55% activity for this construct; however, those values are derived from an end point: cleavage after 2 h at 50 °C. Using data presented in the same paper (Suh et al., 1992), we estimated that the active deleted version cleaves at a rate some 10^3–10^4-fold slower than the SA1-2 precursor that we are using, and perhaps 40–100-fold slower than the nondeleted slow-cleaving ribozyme (HDV133) that they used. These data indicate that, in the small form of the self-cleaving sequence (HDV88), the deleted sequences may be essential, but when the longer form of the precursor (HDV133) is used, either an essential function can be provided by flanking sequences or a less active form of the ribozyme, perhaps missing part of the catalytic center, is stabilized. Although cleavage activity in the deleted form of HDV133 is very low, the possibility that self-cleaving structures could be generated by alternative sequences in the HDV genome could have important implications for self-cleavage in viral replication. It also raises the intriguing possibility that the slower cleavage observed with longer forms of genomic RNA is actually due

to slow-cleaving conformers of the genomic sequence and is not necessarily due to the slow conversion of inactive conformers to the cleavable form.

Stem IV. We had hypothesized that the size of stem IV may mask the effect of a few base changes. This would especially be a problem if, as is almost certainly the case, alternative pairing alignments in the stem were compatible with a self-cleaving structure. Therefore, it was shortened to 4 base pairs but included a stabilizing tetraloop sequence (Tuerk et al., 1988). This shortened version cleaved at least as fast as the original sequence (SA1-2), and mutations in the shortened version were consistent with a requirement for pairing in stem IV. Alterations in the loop sequence had smaller effects on the rate of cleavage (A. T. Perrotta and M. D. Been, unpublished data). If stem IV is replaced by a dinucleotide, the rate of cleavage drops dramatically (dSIVB, Table I). Surprisingly, it still cleaves at about 1% of that of SA1-2 even though this deletion would appear to seriously perturb the geometry of the two strands joining stem IV to stems I and II.

As in the antigenomic sequence, stem IV in the genomic structure has been established as a paired structure that can be replaced with a smaller stem and loop. Although Suh et al. (1992) have deleted most of stem IV in the genomic sequence and report a complete loss of activity, Thill et al. (1991) have made a large but different deletion which could maintain some pairing in stem IV and have found only a small decrease in activity. Thill et al. (1991) did not report any evidence for base-pairing in the remaining portion, but Wu et al. (1992) have made deletions and linker scanner mutations in stem IV of the genomic sequence, and these results are consistent with a requirement for base-pairing.

If stem IV can be shortened considerably without loss of cleavage activity, why then is it conserved as the largest and possibly most stable pairing in the self-cleaving element? Most likely, the in vitro conditions do not accurately represent the in vivo situation, and perhaps a longer stem IV is required for a stable self-cleaving structure in vivo. Likewise, removing the self-cleaving sequence from the remainder of the HDV sequence may obscure a requirement for stem IV in formation of an active ribozyme (Branch & Robertson, 1991). Another possibility is that stem IV serves as a ligand for an RNA binding factor that has some essential role for viral replication.

Application to the Trans-Acting Ribozyme. A trans form of the cleavage reaction in which stem I is generated through an intermolecular association of an enzymatic RNA (ADC1) and a substrate oligoribonucleotide has been described (Perrotta & Been, 1992). CDC200 and PDC7 represent smaller forms of RNA enzymes designed to cleave the same substrate. Each is a composite sequence, differing in regards to which stem, II or IV, is closed by a tetraloop sequence. Introducing a loop at the end of stem II would limit the potential for those sequences to form alternative pairings. Evidence that both forms are active in the trans reaction provides additional support for the overall secondary structure and indicates that a general form of the model can be used in the design of other novel enzymatic RNAs. If HDV ribozymes can be generated from circularly permuted ribozyme sequences, it should be possible to close both stem II and stem IV, thereby making a small circular ribozyme.

Implications for HDV Ribozyme Structure and Function. These studies allow us to make some reasonable predictions and hypotheses about the structure which are consistent with available data or can be tested in further studies. (i) The genomic and antigenomic ribozymes are two versions of the same structural motif. This is illustrated by the generation of novel sequence combinations which have HDV ribozyme-like structures and activity. (ii) Stem I, due to its association with the cleavage site, is involved in cleavage site selection. The trans-acting ribozymes (Perrotta & Been, 1992) provide the best evidence for this, although it can also be tested in the self-cleavage reaction. Target specificity in the trans reaction can be altered with changes to the 3′ side of stem I (Perrotta & Been, 1992). (iii) The lengths of stems I and III are fixed at 7 and 3 base pairs, respectively. The sizes of both are conserved in the genomic and antigenomic elements despite covariance in the sequences. (iv) Stems II and IV have structural roles and serve to constrain the conformational options available to the sequences joining them. The sizes and sequences of stems II and IV can be varied. (v) The region joining stems I and II (JI/II) contains nonessential sequences. The two trans-acting ribozymes suggest this to be the case. (vi) Almost by default, the active site will be formed by specific nucleotides residing in stem loop III and the sequences joining stems I and IV (JI/IV) and stems IV and II (JIV/II). The intermolecular cleavage reaction described by Branch and Robertson (1991) and Wu et al. (1992), if interpreted with our model, would support an essential role for the JIV/II sequence. These three joining sequences are well conserved in the two secondary structures (Figure 1a,b); JI/IV is GGG, JIV/II is GC(U/G)AAg, and stem loop III is UCCUCGCu, where parentheses indicate a variant position and the lower case letter indicates an extra nucleotide in one or the other of the sequences.

ACKNOWLEDGMENT

We thank C. Fierke, D. Herschlag, and M. Puttaraju for comments on the manuscript and C. Fierke also for interest, help, advice, and patience in explaining basic kinetic principles and methods.

REFERENCES

Belinsky, M., & Dinter-Gottlieb, G. (1991) *Nucleic Acids Res. 19*, 559–564.

Branch, A., & Robertson, H. D. (1991) *Proc. Natl. Acad. Sci. U.S.A. 88*, 10163–10167.

Davanloo, P., Rosenberg, A. H., Dunn, J. J., & Studier, F. W. (1984) *Proc. Natl. Acad. Sci. U.S.A. 81*, 2035–2039.

Ehresmann, C., Baudin, F., Mougel, M., Romby, P., Ebel, J. P., & Ehresmann, B. (1987) *Nucleic Acids Res. 15*, 9109–9128.

Feldstein, P. A., Buzayan, J. M., van Tol, H., deBear, J., Gough, G. R., Gilham, P. T., & Bruening, G. (1990) *Proc. Natl. Acad. Sci. U.S.A. 87*, 2623–2627.

Forster, A. C., & Symons, R. H. (1987) *Cell 49*, 211–220.

Freier, S. M., Kierzek, R., Jaeger, J. J., Sugimoto, N., Caruthers, M. H., Neilson, T., & Turner, D. H. (1986) *Proc. Natl. Acad. Sci. U.S.A. 83*, 9373–9377.

Hampel, A., Tritz, R., Hicks, M., & Cruz, P. (1990) *Nucleic Acids Res. 18*, 299–304.

Herschlag, D., & Cech, T. R. (1990) *Biochemistry 29*, 10159–10171.

Hutchins, C. J., Rathjen, P. D., Forster, A. C., & Symons, R. H. (1986) *Nucleic Acids Res. 14*, 3627–3640.

Kunkel, T. A., Roberts, J. D., & Zakour, R. A. (1987) *Methods Enzymol. 154*, 367–382.

Kuo, M. Y.-P., Sharmeen, L., Dinter-Gottlieb, G., & Taylor, J. (1988) *J. Virol. 62*, 4439–4444.

Lowman, H. B., & Draper, D. E. (1986) *J. Biol. Chem. 261*, 5396–5403.

Maniatis, T., Fritsch, E. F., & Sambrook, J. (1982) *Molecular Cloning: A Laboratory Manual*, Cold Spring Harbor University Press, Cold Spring Harbor NY.

Nelson, J. R., & Tinoco, I., Jr. (1982) *Biochemistry 21*, 5289–5295.

Perrotta, A. T., & Been, M. D. (1990) *Nucleic Acids Res. 18*, 6821–6827.

Perrotta, A. T., & Been, M. D. (1991) *Nature 350*, 434–436.

Perrotta, A. T., & Been, M. D. (1992) *Biochemistry 31*, 16–21.

Rosenstein, S. P., & Been, M. D. (1990) *Biochemistry 29*, 8011–8016.

Rosenstein, S. P., & Been, M. D. (1991) *Nucleic Acids Res. 19*, 5409–5416.

Sanger, F., Nicklen, S., & Coulson, A. R. (1977) *Proc. Natl. Acad. Sci. U.S.A. 74*, 5463–5467.

Sharmeen, L., Kuo, M. Y.-P., Dinter-Gottlieb, G., & Taylor, J. (1988) *J. Virol. 62*, 2674–2679.

Smith, J., & Dinter-Gottlieb, G. (1991) *Nucleic Acids Res. 19*, 1285–1289.

Suh, Y.-A., Kumar, P. K. R., Nishikawa, F., Nakai, S., Odai, O., Uesugi, S., Taira, K., & Nishikawa, S. (1992) *Nucleic Acids Res. 20*, 747–753.

Tabor, S., & Richardson, C. C. (1987) *Proc. Natl. Acad. Sci. U.S.A. 84*, 4767–4771.

Thill, G., Blumenfeld, M., Lescure, F., & Vasseur, M. (1991) *Nucleic Acids Res. 19*, 6519–6525.

Tuerk, C., Gayss, P., Thermes, C., Groebe, D. R., Gayle, M., Guild, N., Stormo, G., D'Aubenton-Carafa, Y., Uhlenbeck, O. C., Tinoco, I., Brody, E. N., & Gold, L. (1988) *Proc. Natl. Acad. Sci. U.S.A. 85*, 1364–1368.

Vieira, J., & Messing, J. (1987) *Methods Enzymol. 153*, 3–11.

Wu, H.-N., Lin, Y.-J., Lin, F.-P., Makino, S., Chang, M.-F., & Lai, M. M. C. (1989) *Proc. Natl. Acad. Sci. U.S.A. 86*, 1831–1835.

Wu, H.-N., Wang, Y.-J., Hung, C.-F., Lee, H.-J., & Lai, M. C. C. (1992) *J. Mol. Biol. 223*, 233–245.